Weather and Climate Extremes 48 (2025) 100757

Contents lists available at ScienceDirect

Weather and Climate Extremes

journal homepage: www.elsevier.com/locate/wace

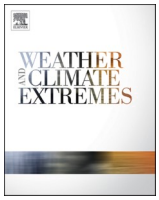

Assessment of the marine heatwaves prediction performance of the short-term climate prediction system FIO-CPS v2.0

Yuanlin Wang [a,b,c], Yajuan Song [a,b,c], Ying Bao [a,b,c], Chan Joo Jang [d], Zhenya Song [a,b,c,*]

[a] First Institute of Oceanography, and Key Laboratory of Marine Science and Numerical Modeling, Ministry of Natural Resources, Qingdao, 266061, China
[b] Laboratory for Regional Oceanography and Numerical Modeling, Qingdao Marine Science and Technology Center, Qingdao, 266237, China
[c] Shandong Key Laboratory of Marine Science and Numerical Modeling, Qingdao, 266061, China
[d] Ocean Circulation and Climate Research Department, Korea Institute of Ocean Science and Technology, Busan, 49111, South Korea

ARTICLE INFO

Keywords:
Short-term climate prediction system
FIO-CPS v2.0
Marine heatwaves

ABSTRACT

In recent years, the frequent occurrence of marine heatwaves (MHWs) has affected the ecological environment and caused considerable socioeconomic impact. Consequently, MHWs prediction has received increasing attention. This study aims to evaluate the short-term (months to interannual timescales) MHWs prediction skill of the First Institute of Oceanography-Climate Prediction System version 2.0 (FIO-CPS v2.0) by using three statistical metrics including symmetric extremal dependence index (SEDI), forecast accuracy (FA), and Brier skill score (BSS). The results revealed that FIO-CPS v2.0 can better predict MHWs in tropical regions, especially in the tropical central and eastern Pacific Ocean, in which the SEDI, FA, and BSS values reached 0.73, 0.92, and 0.27 at the 1-month lead time, respectively. However, the MHWs prediction ability of FIO-CPS v2.0 has spring prediction barriers owing to the driving factors of ENSO. Moreover, further analysis revealed a definite relationship between the ability to predict MHWs and the ability to predict MHWs duration. The prediction skill of FIO-CPS v2.0 appears to be better for long-duration MHWs than for short-duration MHWs. Under the influence of global warming, FIO-CPS v2.0 can reproduce the increase in MHWs duration observed in recent years, and the prediction skill of some regions has been relatively high in the last 15 years. This study deepens the understanding of the prediction ability of FIO-CPS v2.0, and provides an important reference for the application of short-term prediction of MHWs.

1. Introduction

Marine heatwaves (MHWs) are episodes of extreme ocean warming that can persist for days, weeks, or months (Hobday et al., 2016). Occurrences of such events can severely affect the marine ecosystem and the development of fisheries (Smale et al., 2019; Smith et al., 2023; Kajtar et al., 2024) with consequential socioeconomic impacts (Smith et al., 2021). Recently, MHWs have become more common, and the global average MHWs durations have increased compared to those in the 20th century (Oliver et al., 2018). Under the influence of global warming, the ocean temperature will continue to rise, and the duration, intensity, and area of MHWs will continue to increase (Frölicher et al., 2018; Oliver et al., 2019; Darmaraki et al., 2019). Increasing anthropogenic forcings are important factors of MHWs, for example, greenhouse gases lead to longer-lasting, more frequent, and intense MHWs (Ren et al., 2024). Therefore, a better understanding of the physical mechanisms underlying the occurrence and maintenance of MHWs, and improving MHWs prediction are urgently needed (Frölicher and Laufkötter, 2018; Hartog et al., 2023).

Short-term climate prediction, which is known as seasonal forecasting, usually refers to predicting the mean value and variability of meteorological or oceanic variables on monthly to interannual time scales (Dool, 2006; Song et al., 2021). Traditional short-term climate prediction methods include statistical methods and dynamic methods. Statistical methods, such as regression analysis (Mudelsee, 2019), canonical correlation analysis (He and Barnston, 1996), and statistical state-space models (Chen et al., 2019), typically use historical data to discover trends in predictor variables. Dynamic methods are based

* Corresponding author. First Institute of Oceanography, and Key Laboratory of Marine Science and Numerical Modeling, Ministry of Natural Resources, Qingdao, 266061, China.
E-mail address: songroy@fio.org.cn (Z. Song).

https://doi.org/10.1016/j.wace.2025.100757
Received 5 September 2024; Received in revised form 8 February 2025; Accepted 19 February 2025
Available online 20 February 2025

mainly on numerical models and data assimilation systems, and predictions are made by simulating changes and interactions among different climatic spheres. With a deeper understanding of physical processes and the development of science and technology, dynamic-based short-term climate prediction systems have progressed considerably and become the main tool for short-term climate prediction (Johnson et al., 2019; Song et al., 2021).

MHWs are closely related to the sea surface temperature (SST). Therefore, short-term climatic prediction of MHWs can be considered a byproduct of short-term climate prediction of SST (Jacox et al., 2022). Many studies have investigated the prediction of MHWs based on short-term climate prediction systems (Spillman et al., 2021; Jacox et al., 2022; McAdam et al., 2023; de Boisséson and Balmaseda, 2024; Ma et al., 2024). The results revealed that MHWs prediction ability exhibits notable regional differences, with the best performance in the tropical central and eastern Pacific Ocean. Moreover, it has been demonstrated that the monthly data output of short-term climate prediction systems can meet the needs of MHWs prediction (Jacox et al., 2022).

The short-term climate prediction system of the First Institute of Oceanography–Climate Prediction System version 2.0 (FIO-CPS v2.0) is a seasonal prediction system known to perform well in the prediction of SST, El Niño–Southern Oscillation (ENSO), and 2-m air temperature (Song et al., 2021; Fu et al., 2023); however, its ability to predict MHWs remains unclear. This study evaluated the ability of FIO-CPS v2.0 to predict MHWs and analyzed the prediction bias, thereby providing a basis for further improvement of the prediction ability of the system. Section 2 introduces the model, data, and methods used in this study. Section 3 analyzes the MHWs prediction ability of FIO-CPS v2.0, with assessment results presented in Section 3.1 and a discussion provided in Section 3.2. Finally, Section 4 presents the conclusions of this study.

2. Data and methods

2.1. FIO-CPS v2.0

FIO-CPS v2.0 comprises an assimilation module that uses the nudging method to assimilate SST data and the climate model named FIO-ESM v2.0 (First Institute of Oceanography-Earth System Model version 2.0), which features coupled ocean surface waves and considers unique physical processes such as wave-induced mixing, Stokes drift, sea spray, and diurnal variations in SST (Bao et al., 2020).

For the period 1948–1981, the data assimilated by FIO-CPS v2.0 comprised the Centennial in situ Observation-Based Estimates of daily SST with 1° × 1° resolution (Hirahara et al., 2014). Since 1982, the daily Optimum Interpolation SST (OISST) v2.1 data with 0.25° × 0.25° resolution have been assimilated (Banzon et al., 2020).

Each FIO-CPS v2.0 prediction provides results for the subsequent 13 months and contains 10 ensemble members. This study used global monthly prediction SST data for 1991–2024, with a 1.1° × (0.27–0.54°) resolution. For convenience of comparison, the data were interpolated to the 1° × 1° resolution.

2.2. OISST v2.1

OISST v2.1 is a dataset released by NOAA, which is based on the optimal interpolation method. In this study, OISST v2.1 monthly SST data were used to determine the observation results of MHWs. The period of 1991–2024 was selected to be the same as that of FIO-CPS v2.0, and the data were also interpolated to the 1° × 1° resolution. The URL for downloading the data is as follows: https://psl.noaa.gov/data/gridded/data.noaa.oisst.v2.highres.html.

2.3. Methods for determining MHWs

To determine the MHWs, this study used the method proposed by Hobday et al. (2016), which was adjusted for monthly data (Jacox et al., 2020). First, SST anomalies were calculated based on the monthly climatology for 1991–2024. Second, the MHWs threshold for each month was selected based on the 90th percentile of the SST anomaly for 3 consecutive months. For example, for March, the MHWs threshold is the 90th percentile SST anomaly of ten ensemble members from February-March-April in 1991–2024. Finally, the SST anomalies were compared with their respective thresholds, and the SST anomalies were converted into a binary time series of occurrence and nonoccurrence of MHWs. Therefore, there are four possible predictions: true positive (TP), when MHWs are predicted and do occur; false positive (FP), when MHWs are predicted but do not occur; false negative (FN), when MHWs are not predicted but do occur; and true negative (TN), when MHWs are not predicted and do not occur. Additionally, the prediction probability, ranging from 0 to 1, is the proportion of ensemble members predicting a MHWs, which is taken as the average of the binary time series (MHWs occurrence is 1, MHWs nonoccurrence is 0) from all ensemble members. Notably, this method can only predict the occurrence, duration, and intensity of MHWs on a scale longer than a month.

2.4. Prediction reference baseline

For the evaluation criteria of prediction ability, we used random prediction and persistence prediction as reference baselines.

2.4.1. Random prediction

Random prediction uses statistics and probability theory, in combination with historical data and current observational data, to predict the future state of atmospheric and oceanic systems. For an asymptotically fair evaluation indicator, the expected value represents the random prediction (Gandin and Murphy, 1992):

$$MHWs_{ran} = f(x_1, x_2, \bullet\bullet\bullet, x_n) \tag{1}$$

where $MHWs_{ran}$ is the MHWs random prediction, x_1, x_2, …, x_n are the different data sources, and f is a variety of statistical and probabilistic methods.

2.4.2. Persistence prediction

Persistence prediction uses the situation in the current month as the prediction result (Knaff and Landsea, 1997). The duration of MHWs is an important factor affecting prediction. Persistence prediction has a clear advantage in simulating MHWs with long duration. For example, studies have shown that the result of persistence prediction within a 3-month lead time is better than that of most prediction strategies (Barnston et al., 1994; Latif et al., 1998; Goddard et al., 2001), and some earlier studies have used persistence prediction as a reference prediction (Mason and Mimmack, 2002; Jacox et al., 2019b):

$$MHWs_{per}(i,t) = MHWs_{obs}(i-t) \tag{2}$$

where $MHWs_{per}$ is the MHWs persistence prediction, $MHWs_{obs}$ is the MHWs observation, t is the lead time from 1 month to 13 months, and i is the time series.

2.5. Statistical indicators for prediction skill assessment

This study used the symmetric extremal dependence index (SEDI), forecast accuracy (FA), and Brier skill score (BSS) (Brier, 1950; Jacox et al., 2022; Sun et al., 2023) to evaluate the accuracy and probability of MHWs produced by FIO-CPS v2.0. These three indicators can better reflect the assessment of extreme events than traditional indicators.

2.5.1. SEDI

SEDI is an important indicator used to assess the prediction ability of extreme climate events, and it has the characteristics of nondegenerate, base rate independence, asymptotic fairness, and difficulty hedging

(Ferro and Stephenson, 2011). To calculate the SEDI, the hit rate (H) and the false alarm rate (F) are first determined, where H is the proportion of the predicted MHWs in occurrence (Eq. (3)) and F is the proportion of the predicted MHWs in nonoccurrence (Eq. (4)):

$$H = \frac{TP}{TP + FN} \tag{3}$$

$$F = \frac{FP}{FP + TN} \tag{4}$$

$$SEDI = \frac{\log(F) - \log(H) - \log(1-F) + \log(1-H)}{\log(F) + \log(H) + \log(1-F) + \log(1-H)} \tag{5}$$

SEDI can be calculated using H and F (Eq. (5)). The range of SEDI values is [−1, 1]. A value of SEDI that is higher (lower) than 0 indicates that the prediction ability is better (lower) than that of random prediction.

2.5.2. FA

FA assesses the correct part of the prediction such that the prediction ability is presented as a percentage:

$$FA = \frac{TP + TN}{TP + FP + FN + TN} \tag{6}$$

In this study, MHWs were considered events with a 10% probability of occurrence, and an expected FA of 0.82. Therefore, a value of FA higher (lower) than 0.82 indicates that the prediction ability is better (lower) than that of random prediction.

2.5.3. BSS

BSS mainly evaluates the prediction probability. BSS is calculated using the Brier score (BrS), which is an estimate of the mean square error of the prediction probability:

$$BrS = \frac{1}{N}\sum_{i=1}^{N}(f_i - o_i)^2 \tag{7}$$

where f_i is the predicted probability of FIO-CPS v2.0 and o_i is a binary variable of the observational data. BrS is then normalized relative to the reference prediction (BrSref). BrSref is the time series mean of prediction probability, which is close to 0.1. The BSS can be expressed as follows:

$$BSS = 1 - \frac{BrS}{BrS_{ref}} \tag{8}$$

BSS is an assessment indicator based on the prediction probability that can explain the difference between the predicted results and observed results. BSS is very sensitive to prediction bias, and it can capture the effects of prediction bias and uncertainty. The range of the BSS is [−∞, 1]. A BSS value higher (lower) than 0 indicates that the prediction ability is better (lower) than that of random prediction.

3. Results and Discussions

3.1. Evaluation of MHWs prediction ability

Fig. 1 shows the spatial distributions of the three evaluation indicators. Generally, the MHWs prediction ability of FIO-CPS v2.0 shows considerable regional differences, being better in the tropics and poorer in the regions of the western boundary currents and the Southern Ocean. However, the prediction ability indicated by both the SEDI (Fig. 1a, d, and g) and FA (Fig. 1b, e, and h) is better than that indicated by the BSS (Fig. 1c, f, and i) because the responses of the indicators to prediction bias are different. According to the statistical results, the number of TNs is large compared with that of the other three events, resulting in higher values of the SEDI and FA. In contrast, TN has a lesser effect on the BSS, meaning that the ability of the BSS to indicate the deviation is stronger.

For the tropical central and eastern Pacific Ocean, the SEDI, FA, and BSS values at a 1-month lead time reach 0.73, 0.92, and 0.27, respectively, and decrease with increasing lead time. For extratropical regions, although the SEDI and FA values decrease as the lead time increases, the BSS does not diminish with increasing lead time. At the 1-month lead time, the areas where the BSS indicates prediction ability that is worse

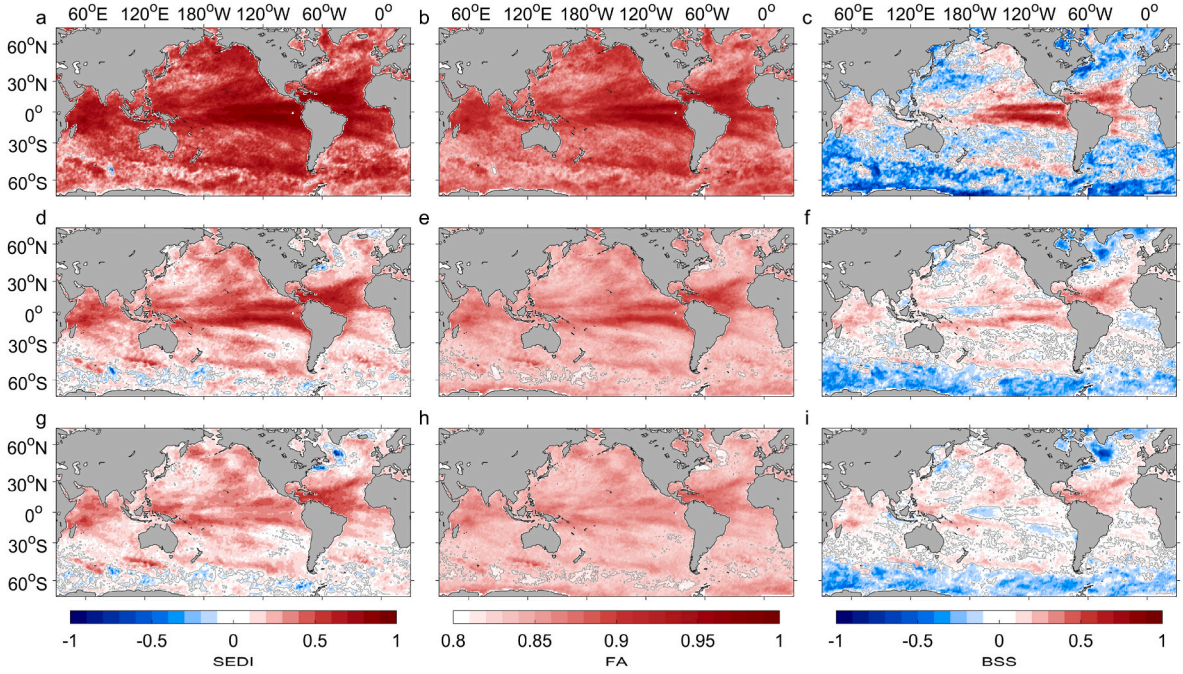

Fig. 1. Spatial distribution of indicators for assessing the ability of the FIO-CPS v2.0 to predict MHWs. (a, d, g) Spatial distribution of the SEDI. The gray solid line indicates that the MHWs prediction of FIO-CPS v2.0 is comparable to that of random prediction, and the value is 0. (b, e, h) Spatial distribution of the FA. The value of the gray solid line is 0.82. (c, f, i) Spatial distribution of the BSS. The value of the gray solid line is 0. (a–c) 1-month lead time, (d–f) 5-month lead time, and (g–i) 9-month lead time.

than that of random prediction are the most common among all lead times, and the prediction deviation is the most obvious in western boundary currents and Southern Ocean regions. This might be due to the large degree of dispersion of the prediction probability at short lead times, which leads to a greater BrS and a smaller BSS. However, this does not mean that the prediction ability is better at long lead times.

To further analyze the MHWs prediction bias of FIO-CPS v2.0 at short lead times, we introduced the persistence prediction as the reference prediction baseline. Because the observational data (OISST v2.1) cannot reflect the prediction probability, the BSS of the persistence prediction cannot be calculated. Therefore, we calculated only the SEDI and FA scores of the persistence prediction for comparison with those of FIO-CPS v2.0. Owing to the presence of permanent or seasonal sea ice at high latitudes, only regional averages of 60°S–60°N were used to analyze the changes in the assessment indicators globally (Fig. 2a–c). At short lead time, the SEDI values of FIO-CPS v2.0 are lower than those of the persistence prediction, which is consistent with the trend of the BSS. The FA of FIO-CPS v2.0 are lower than those of the persistence at all lead times in the region of 60°S-60°N. The BSS is relatively poor at short lead times. In fact, for short lead times, the prediction ability of FIO-CPS v2.0 is lower than that of the persistence prediction, especially in extra-tropical regions; however, in the tropics, the prediction ability of FIO-CPS v2.0 is equivalent to or better than that of the persistence prediction. The BSS corresponding to those areas is better than the random prediction ability, e.g., the tropical central and eastern Pacific Ocean (20°S–20°N, 80°–180°W; Fig. 2f), the tropical Indian Ocean (20°S–20°N, 60°–90°E; Fig. 2i), and the tropical Atlantic Ocean (20°S–20°N, 0°–60°W; Fig. 2l).

The MHWs prediction ability was analyzed from the perspective of target months. Because MHWs are extreme climatic events and the total number of MHWs is limited, when analyzing the MHWs prediction ability in target months, limiting the number of MHWs in each month will lead to a lower SEDI value, a larger FA value, and a BSS tending toward negative infinity. In comparison, the variation range of the FA is small, and there are some meaningless BSS values. Therefore, the SEDI can better show the relationship between the prediction ability and the target months. Globally (Fig. 3a), the SEDI is less than 0 at most lead times, and it is better than the random prediction only at 1- and 2-month lead times. Indeed, the result for extratropical regions is better than random prediction only at 1-month lead time. Over the tropical central and eastern Pacific Ocean (Fig. 3b), the SEDI is relatively poor in reflecting the ability to predict MHWs between May and July, and the poor prediction ability gradually extends to later months with increasing lead times. This trend is similar to the results of SST in the ENSO region (Song et al., 2021). These findings indicate that MHWs prediction has spring prediction barriers, and that ENSO might be an important driving

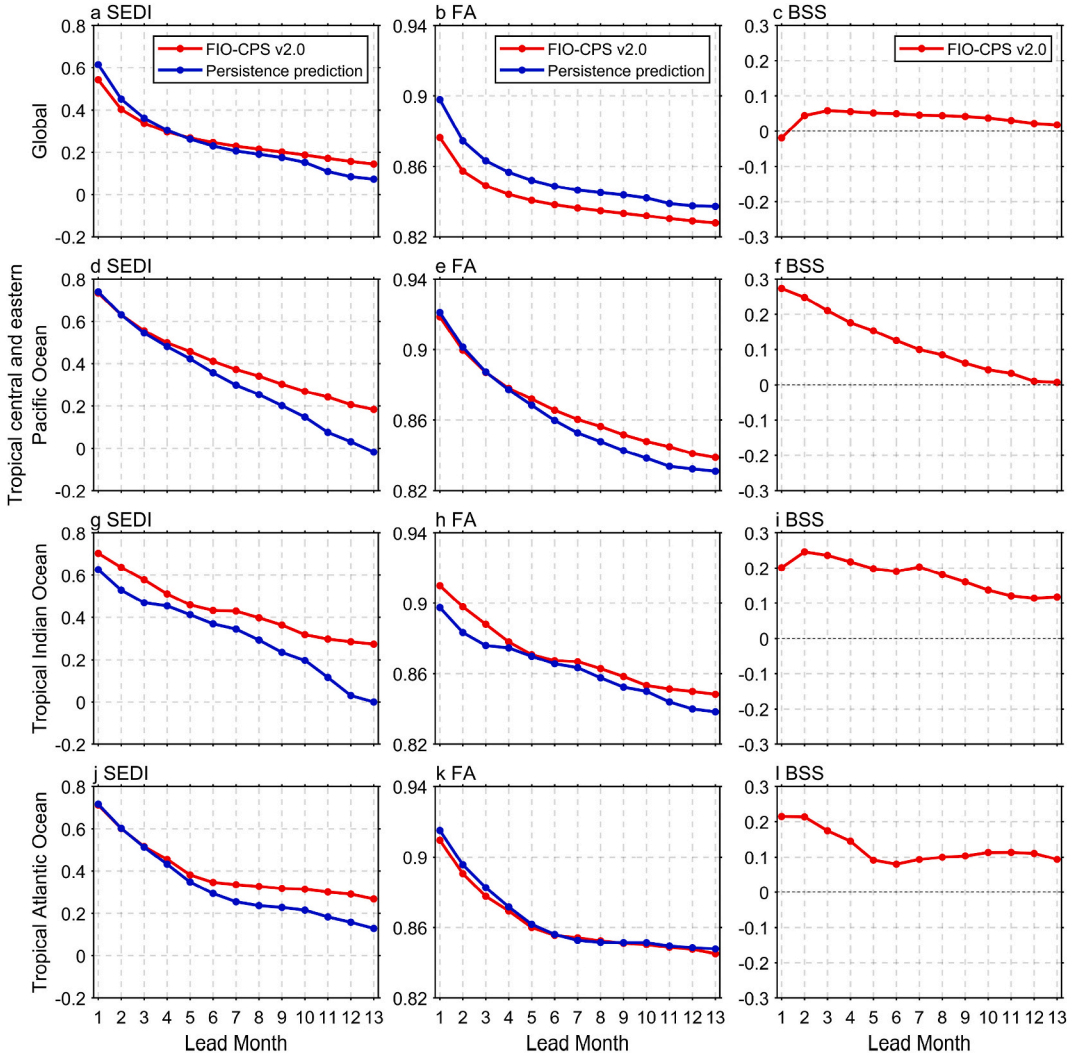

Fig. 2. Changes in the regional mean of the assessment indicators with lead time: (a–c) global mean of the assessment indicators, (d–f) regional mean of the tropical central and eastern Pacific Ocean, (g–i) regional mean of the tropical Indian Ocean, and (j–l) regional mean of the tropical Atlantic Ocean. Red solid line is the result of FIO-CPS v2.0, and blue solid line is the result of the persistence prediction.

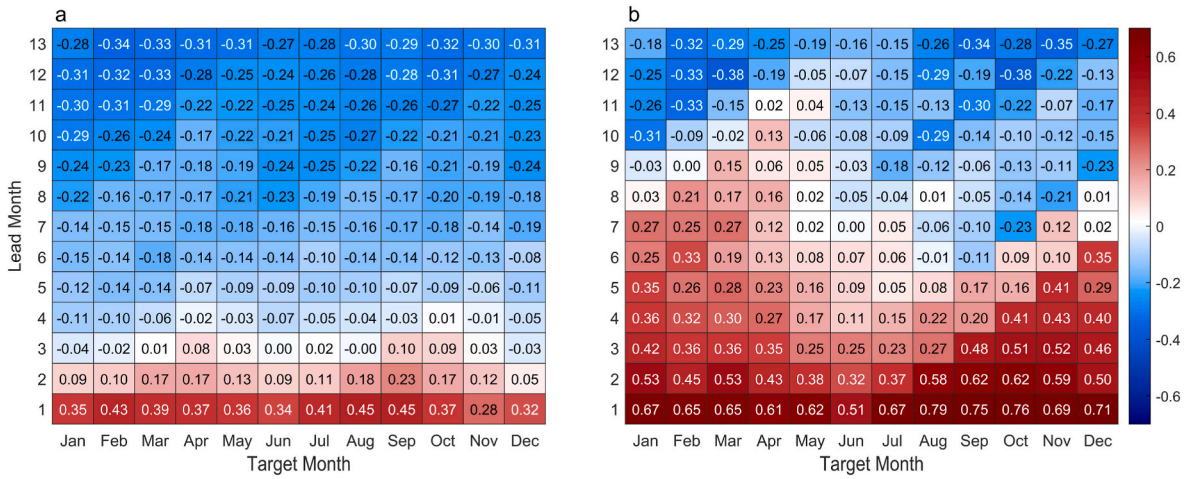

Fig. 3. Relationships among prediction ability, lead time, and target month: (a) global mean (60°S–60°N) and (b) regional mean for the tropical central and eastern Pacific Ocean (20°S–20°N, 80°–180°W).

factor of MHWs.

3.2. Discussions on MHWs prediction ability

The assessment results show substantial regional differences in the MHWs prediction ability of FIO-CPS v2.0, which are better in the tropics and poorer in extratropical regions. In fact, the prediction skill is related to the characteristics of MHWs. We found that the spatial distributions of the MHWs annual frequency (Fig. 4a, d, and g) and annual mean duration (Fig. 4b, e, and h) are similar to those of the MHWs prediction ability. The annual frequency, the number of MHWs occurrences per year, calculated from the monthly data is less than that calculated from the daily data. The duration, the time between the start month and the end month of the MHWs, estimated from the monthly data is greater than that of the daily data, because MHWs with duration of less than 1 month are either ignored or determined to have duration of 1 month. However, the spatial distributions of the monthly data are similar to those of the daily data. The frequency of MHWs in the tropics is low, and their duration is long (Oliver et al., 2018; Holbrook et al., 2020), particularly in the tropical central and eastern Pacific Ocean. With a 1-month lead time, the frequency reaches 0.3, and the duration reaches 5 months, indicating that this type of MHWs has the highest prediction ability (Jacox et al., 2022). The prediction ability of FIO-CPS v2.0 is also the best with a 1-month lead time. In areas with poor prediction ability, particularly in the region of western boundary currents and the Southern Ocean, MHWs are high in frequency and short in duration. High-energy, complex, and changeable ocean currents increase the difficulty of MHWs prediction (Holbrook et al., 2019; Jacox et al., 2020). For the annual mean intensity of MHWs (Fig. 4c, f, and i), in the tropics, the ability to predict high-intensity MHWs in the tropical central and eastern Pacific

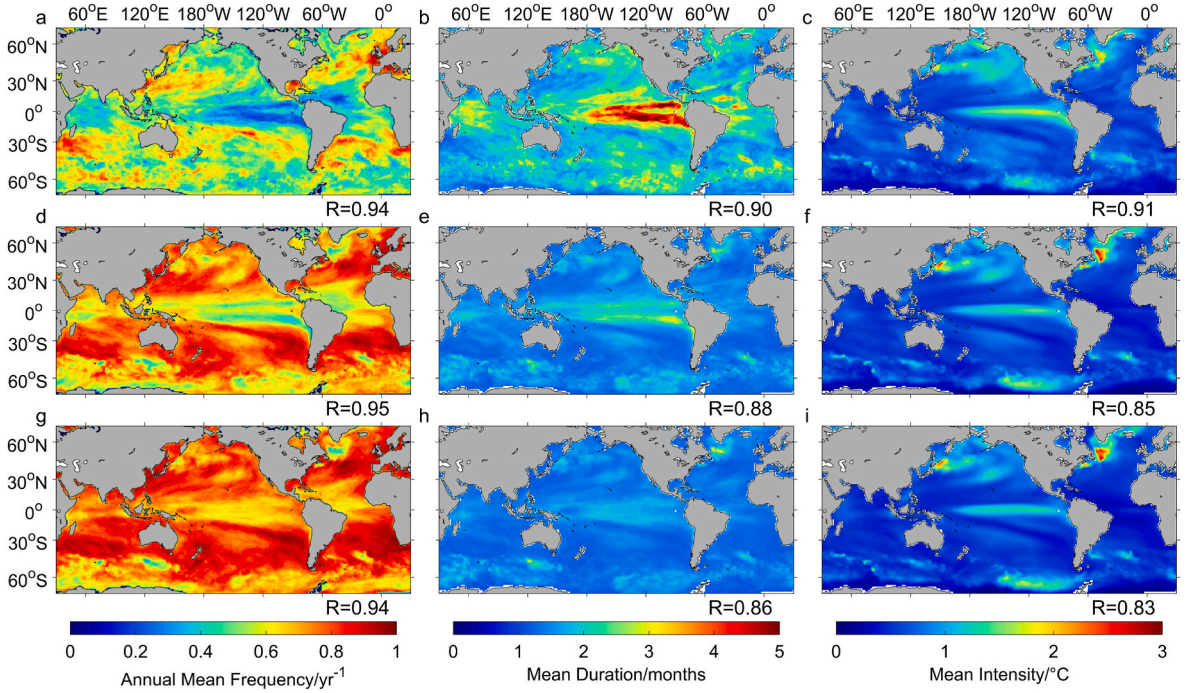

Fig. 4. Spatial distributions of the annual frequency, annual mean duration, and annual mean intensity of MHWs simulated by FIO-CPS v2.0: (a, d, g) annual frequency of MHWs, (b, e, h) mean duration of MHWs, and (c, f, i) mean intensity of MHWs. (a–c) 1-month lead time, (d–f) 5-month lead time, and (g–i) 9-month lead time. The R value is the Pearson correlation coefficient between FIO-CPS v2.0 and the observational data between 60°S and 60°N.

Ocean is better than that of minor-intensity MHWs in the tropical Indian Ocean and the tropical Atlantic Ocean. High-intensity MHWs indicate greater chances of long-duration MHWs, however, for regions with complex and variable influencing factors, such as the western boundary current, high-intensity MHWs will increase the difficulty of prediction. Therefore, high intensity is a necessary condition for a long duration. In addition, the Atlantic meridional overturning circulation (AMOC) is an important factor that contributes to the spatial distribution of MHWs properties. A weaken AMOC leads to higher intensity and annual frequency in the south of Greenland (Ren and Liu, 2021). The above analysis reveals that the prediction ability of MHWs has a corresponding relationship with their frequency and duration, and that FIO-CPS v2.0 has greater prediction ability for MHWs with low frequency and long duration.

As the lead time increases, the frequency of MHWs increases (Fig. 5b), and the duration decreases (Fig. 5c). This can explain the diminished prediction ability in the tropics, but not the poor prediction ability at short lead times in extratropical regions. Further analysis reveals that the dispersion degree of the prediction probability is excessively large at a 1-month lead time (bars in Fig. 6). As the lead time increases, the dispersion degree of the prediction probability decreases (not shown), resulting in the BrS smaller, which in turn leads to a larger BSS. However, this does not mean that the prediction ability is better at long lead times. In fact, the MHWs characteristics simulated by FIO-CPS v2.0 are strongly correlated with the observational data at short lead times (Fig. 4). Owing to the high frequency and short duration of MHWs, the prediction bias of FIO-CPS v2.0 is substantial in extratropical regions.

Prediction skills of the frequency, duration, and intensity of MHWs depend on the simulation ability of the driving factors (Jacox et al., 2019b). For example, in the tropical central and eastern Pacific Ocean (Fig. 6a), the FIO-CPS v2.0 predicts two MHWs from 1997 to 1998 and 2015 to 2016 with a duration of 9 and 10 months, respectively. These events are accompanied by two high-intensity El Niño events, whereas other short-duration MHWs are accompanied by lower-intensity El Niño events, and the prediction deviations occur mainly in relatively short-duration MHWs. Therefore, the MHWs prediction ability in this region depends mainly on the ENSO prediction ability. However, as the lead time increases, the prediction ability of ENSO decreases, leading to an increase in the prediction bias of MHWs. For the other four locations, under the influence of global warming, we found that the duration of MHWs in the last 15 years becomes longer. And the statistical results show that the mean duration of MHWs after 2010 is greater than that before 2010. In the tropical Indian Ocean (Fig. 6b), the SEDI is relatively large after 2010 on the basis of the calculations; therefore, the prediction deviations appear mainly during the short-duration MHWs before 2010. In the tropical Atlantic Ocean (Fig. 6c), the SEDI is slightly larger after 2010, and FIO-CPS v2.0 is accurate in predicting several long-duration MHWs after 2010. In the northeastern Pacific Ocean (Fig. 6d), FIO-CPS v2.0 predicts MHWs that occur mainly during the positive phase of the Pacific Decadal Oscillation. Among them, the 2013–2016 MHWs, known as “the Blob”, produced several consecutive long MHWs in the northeastern Pacific Ocean, and its central location and driving factors have changed. As the center of “the Blob” moved toward the coast (Amaya et al., 2016), the driving factors includes air-sea heat flux anomalies, wind drivers and so on (Bond et al., 2015; Di Lorenzo and

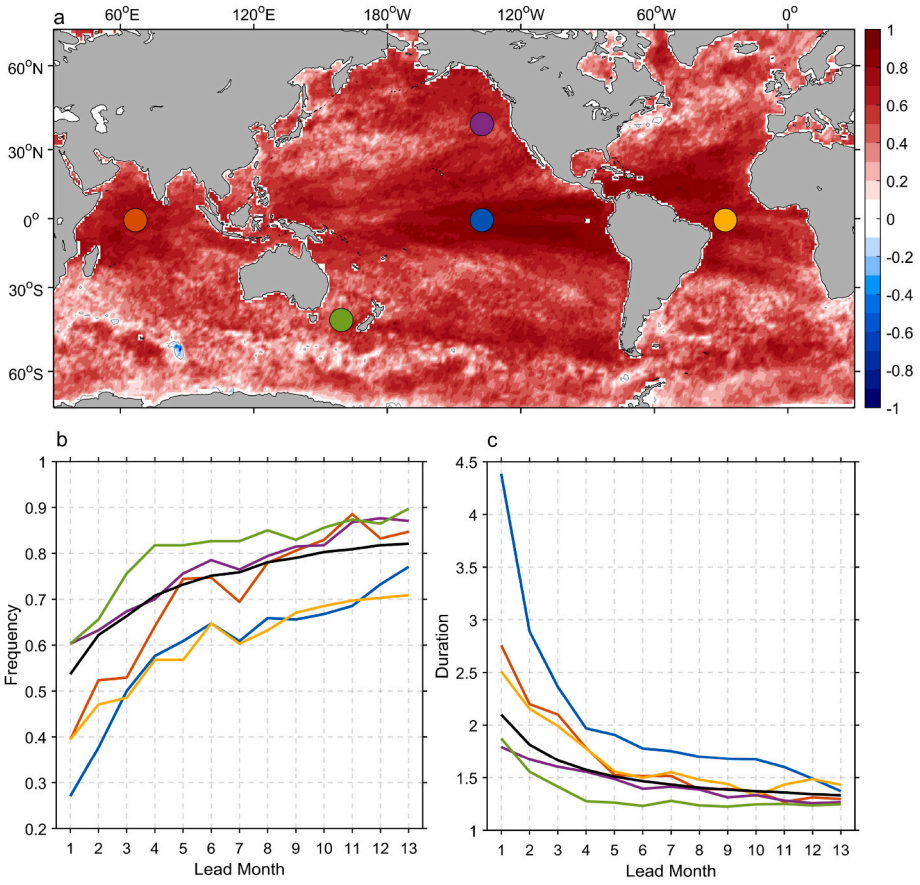

Fig. 5. Lead time series of the frequency and duration of MHWs at five locations: (a) SEDI at 1-month lead time, (b) lead time series of the annual mean frequency of MHWs, and (c) lead time series of the annual mean duration of MHWs. The five locations are the tropical central and eastern Pacific Ocean (blue circle and line), tropical Indian Ocean (orange circle and line), tropical Atlantic Ocean (yellow circle and line), Northeast Pacific Ocean (purple circle and line), and Tasman Sea (green circle and line). Black lines in (b) and (c) are the global spatial mean (60°S–60°N).

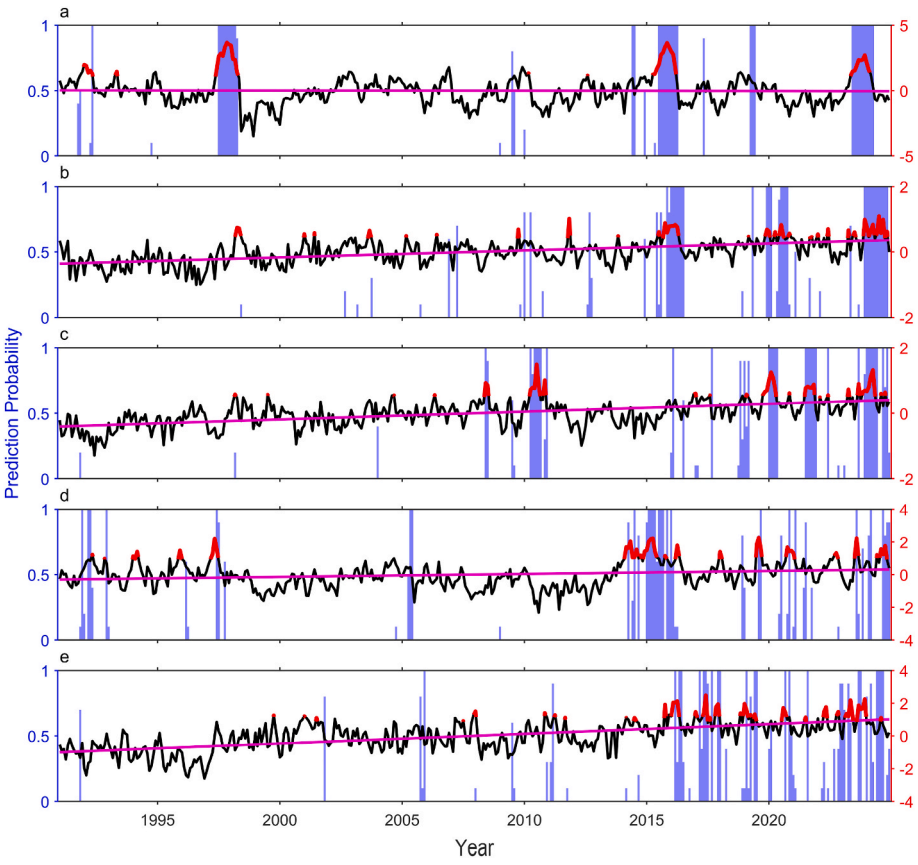

Fig. 6. Observational data at five locations and the time series of MHWs from FIO-CPS v2.0: (a–e) SST anomaly of the observational data (solid black line), MHWs of the observational data (solid red line), and prediction probability of FIO-CPS v2.0 at a 1-month lead time (blue bars). The solid pink line is the SST anomaly trend. The specific locations are shown in Fig. 5(a). (a) tropical central and eastern Pacific Ocean; (b) tropical Indian Ocean; (c) tropical Atlantic Ocean; (d) Northeast Pacific Ocean; and (e) Tasman Sea.

Mantua, 2016; Hu et al., 2017). Large-scale climate modes, such as the ENSO and pacific decadal oscillation (PDO), also have significant impacts (Jacox et al., 2019a; Ren et al., 2023). FIO-CPS v2.0 successfully predicts "the Blob" with long durations, but there are deviations in time and space. Additionally, in the Tasman Sea (Fig. 6e), FIO-CPS v2.0 predicts MHWs caused by ocean heat transport during 2015–2016 (Oliver et al., 2017) and MHWs caused by air–sea heat flux during 2017–2018 (Perkins-Kirkpatrick et al., 2019; Kajtar et al., 2022). Similarly, for these two locations, the duration of MHWs increased after 2010, which might be related to the effect of global warming (Kajtar et al., 2021), and the SEDI was also relatively large after 2010, so the prediction ability of FIO-CPS v2.0 was more accurate in the later period than in the earlier period. In the five locations, the FIO-CPS v2.0 is more accurate in predicting long-duration MHWs. Generally, the duration of MHWs is increasing under the influence of global warming, and the MHWs prediction ability of FIO-CPS v2.0 can provide an important research basis.

4. Conclusions

This study evaluated MHWs prediction by the FIO-CPS v2.0 short-term climate prediction system across different regions, varying lead times, and different target months. The results indicate that the MHWs prediction skill of FIO-CPS v2.0 has significant regional differences, which are higher in tropical regions and lower in extratropical regions. This regional difference is attributable to the low frequency and long duration of MHWs in the tropics, particularly in the tropical central and eastern Pacific Ocean. In extratropical regions, the prediction deviation of FIO-CPS v2.0 occurs mainly during short-duration MHWs. Under the influence of global warming, FIO-CPS v2.0 can reproduce the increase in MHWs duration observed in recent years, and the prediction skill of some regions is relatively high in the last 15 years. Additionally, we found that the MHWs prediction ability also has spring prediction barrier, similar to the ENSO prediction, which indicates that ENSO influences MHWs in the tropical central and eastern Pacific directly, and other regions through teleconnection.

In this study, monthly data was used for the analysis of MHWs prediction by FIO-CPS v2.0. There are a large number of MHWs with durations of less than 1 month, and these signals may be ignored in monthly data. Furthermore, future work should benefit greatly by using high resolution model for MHWs prediction because the ocean current energy in the regions of the western boundary currents and Southern Ocean is very important.

CRediT authorship contribution statement

Yuanlin Wang: Writing – original draft, Visualization, Methodology, Investigation, Formal analysis. **Yajuan Song:** Writing – review & editing, Validation, Methodology, Data curation. **Ying Bao:** Writing – review & editing, Validation, Methodology. **Chan Joo Jang:** Writing – review & editing, Validation. **Zhenya Song:** Writing – review & editing, Supervision, Project administration, Methodology, Funding acquisition, Formal analysis, Conceptualization.

Declaration of competing interest

The authors declare that they have no known competing financial interests or personal relationships that could have appeared to influence

the work reported in this paper.

Acknowledgments

This work was supported by the National Natural Science Foundation of China (42425606), Basic Scientific Fund for the National Public Research Institute of China (Shu-Xingbei Young Talent Program 2023S01), Laoshan Laboratory (LSKJ202202100), Ocean Decade International Cooperation Center Scientific and Technological Cooperation Projects (GHKJ2024005), and China-Korea Joint Ocean Research Center (CN: PI-20240101, KR: 20220407).

Data availability

Data will be made available on request.

References

Amaya, D., Bond, N., Miller, A., DeFlorio, M., 2016. The evolution and known atmospheric forcing mechanisms behind the 2013-2015 North Pacific warm anomalies. CLIVAR's Variations Newsletter Spring 1–6.

Banzon, V., Smith, T.M., Steele, M., Huang, B., Zhang, H.-M., 2020. Improved estimation of proxy sea surface temperature in the arctic. J. Atmos. Ocean. Technol. 37, 341–349. https://doi.org/10.1175/JTECH-D-19-0177.1.

Bao, Y., Song, Z., Qiao, F., 2020. FIO-ESM version 2.0: model description and evaluation. J. Geophys. Res.: Oceans 125, e2019JC016036. https://doi.org/10.1029/2019JC016036.

Barnston, A.G., Dool, H.M. van den, Zebiak, S.E., Barnett, T.P., Ji, M., Rodenhuis, D.R., Cane, M.A., Leetmaa, A., Graham, N.E., Ropelewski, C.R., Kousky, V.E., O'Lenic, E. A., Livezey, R.E., 1994. Long-lead seasonal forecasts—where do we stand? Bull. Am. Meteorol. Soc. 75, 2097–2114. https://doi.org/10.1175/1520-0477(1994)075<2097:LLSFDW>2.0.CO;2.

Bond, N.A., Cronin, M.F., Freeland, H., Mantua, N., 2015. Causes and impacts of the 2014 warm anomaly in the NE Pacific. Geophys. Res. Lett. 42, 3414–3420. https://doi.org/10.1002/2015GL063306.

Brier, G.W., 1950. Verification of forecasts expressed in terms of probability. Mon. Weather Rev. 78, 1–3. https://doi.org/10.1175/1520-0493(1950)078<0001:VOFEIT>2.0.CO;2.

Chen, C.-C., Wang, Y.-R., Guo, Y.-L.L., Wang, Y.-C., Lu, M.-M., 2019. Short-term prediction of extremely hot days in summer due to climate change and ENSO and related attributable mortality. Sci. Total Environ. 661, 10–17. https://doi.org/10.1016/j.scitotenv.2019.01.168.

Darmaraki, S., Somot, S., Sevault, F., Nabat, P., Cabos Narvaez, W.D., Cavicchia, L., Djurdjevic, V., Li, L., Sannino, G., Sein, D.V., 2019. Future evolution of marine heatwaves in the mediterranean sea. Clim. Dyn. 53, 1371–1392. https://doi.org/10.1007/s00382-019-04661-z.

de Boisséson, E., Balmaseda, M.A., 2024. Predictability of marine heatwaves: assessment based on the ECMWF seasonal forecast system. Ocean Sci. 20, 265–278. https://doi.org/10.5194/os-20-265-2024.

Di Lorenzo, E., Mantua, N., 2016. Multi-year persistence of the 2014/15 North Pacific marine heatwave. Nat. Clim. Change 6, 1042–1047. https://doi.org/10.1038/nclimate3082.

Dool, den, H.M.V., 2006. Empirical Methods in Short-Term Climate Prediction. Oxford University Press. https://doi.org/10.1093/OSO/9780199202782.001.0001.

Ferro, C.A.T., Stephenson, D.B., 2011. Extremal dependence indices: improved verification measures for deterministic forecasts of rare binary events. Weather Forecast. 26, 699–713. https://doi.org/10.1175/WAF-D-10-05030.1.

Frölicher, T.L., Fischer, E.M., Gruber, N., 2018. Marine heatwaves under global warming. Nature 560, 360–364. https://doi.org/10.1038/s41586-018-0383-9.

Frölicher, T.L., Laufkötter, C., 2018. Emerging risks from marine heat waves. Nat. Commun. 9, 650. https://doi.org/10.1038/s41467-018-03163-6.

Fu, Q., Song, Z., Bo, Z., Bao, Y., Jang, C.J., Song, Y., 2023. Assessment of the FIO-CPS v2.0 in predicting 2-meter air temperature over China. Dynam. Atmos. Oceans 103, 101391. https://doi.org/10.1016/j.dynatmoce.2023.101391.

Gandin, L.S., Murphy, A.H., 1992. Equitable skill scores for categorical forecasts. Mon. Weather Rev. 120, 361–370. https://doi.org/10.1175/1520-0493(1992)120<0361:ESSFCF>2.0.CO;2.

Goddard, L., Mason, S.j., Zebiak, S.e., Ropelewski, C.f., Basher, R., Cane, M.a., 2001. Current approaches to seasonal to interannual climate predictions. Int. J. Climatol. 21, 1111–1152. https://doi.org/10.1002/joc.636.

Hartog, J.R., Spillman, C.M., Smith, G., Hobday, A.J., 2023. Forecasts of marine heatwaves for marine industries: reducing risk, building resilience and enhancing management responses. Deep Sea Res. Part II Top. Stud. Oceanogr. 209, 105276. https://doi.org/10.1016/j.dsr2.2023.105276.

He, Y., Barnston, A.G., 1996. Long-lead forecasts of seasonal precipitation in the tropical pacific islands using CCA. J. Clim. 9, 2020–2035.

Hirahara, S., Ishii, M., Fukuda, Y., 2014. Centennial-scale sea surface temperature analysis and its uncertainty. J. Clim. 27, 57–75. https://doi.org/10.1175/JCLI-D-12-00837.1.

Hobday, A.J., Alexander, L.V., Perkins, S.E., Smale, D.A., Straub, S.C., Oliver, E.C.J., Benthuysen, J.A., Burrows, M.T., Donat, M.G., Feng, M., Holbrook, N.J., Moore, P.J., Scannell, H.A., Sen Gupta, A., Wernberg, T., 2016. A hierarchical approach to defining marine heatwaves. Prog. Oceanogr. 141, 227–238. https://doi.org/10.1016/j.pocean.2015.12.014.

Holbrook, N.J., Claar, D.C., Hobday, A.J., McInnes, K.L., Oliver, E.C.J., Gupta, A.S., Widlansky, M.J., Zhang, X., 2020. ENSO-driven ocean extremes and their ecosystem impacts. In: El Niño Southern Oscillation in a Changing Climate. American Geophysical Union (AGU), pp. 409–428. https://doi.org/10.1002/9781119548164.ch18.

Holbrook, N.J., Scannell, H.A., Sen Gupta, A., Benthuysen, J.A., Feng, M., Oliver, E.C.J., Alexander, L.V., Burrows, M.T., Donat, M.G., Hobday, A.J., Moore, P.J., Perkins-Kirkpatrick, S.E., Smale, D.A., Straub, S.C., Wernberg, T., 2019. A global assessment of marine heatwaves and their drivers. Nat. Commun. 10, 2624. https://doi.org/10.1038/s41467-019-10206-z.

Hu, Z.-Z., Kumar, A., Jha, B., Zhu, J., Huang, B., 2017. Persistence and predictions of the remarkable warm anomaly in the northeastern Pacific Ocean during 2014–16. J. Clim. 30, 689–702. https://doi.org/10.1175/JCLI-D-16-0348.1.

Jacox, M.G., Alexander, M.A., Amaya, D., Becker, E., Bograd, S.J., Brodie, S., Hazen, E.L., Pozo Buil, M., Tommasi, D., 2022. Global seasonal forecasts of marine heatwaves. Nature 604, 486–490. https://doi.org/10.1038/s41586-022-04573-9.

Jacox, M.G., Alexander, M.A., Bograd, S.J., Scott, J.D., 2020. Thermal displacement by marine heatwaves. Nature 584, 82–86. https://doi.org/10.1038/s41586-020-2534-z.

Jacox, M.G., Alexander, M.A., Stock, C.A., Hervieux, G., 2019a. On the skill of seasonal sea surface temperature forecasts in the California Current System and its connection to ENSO variability. Clim. Dyn. 53, 7519–7533. https://doi.org/10.1007/s00382-017-3608-y.

Jacox, M.G., Tommasi, D., Alexander, M.A., Hervieux, G., Stock, C.A., 2019b. Predicting the evolution of the 2014–2016 California current system marine heatwave from an ensemble of coupled global climate forecasts. Front. Mar. Sci. 6. https://doi.org/10.3389/fmars.2019.00497.

Johnson, S.J., Stockdale, T.N., Ferranti, L., Balmaseda, M.A., Molteni, F., Magnusson, L., Tietsche, S., Decremer, D., Weisheimer, A., Balsamo, G., Keeley, S.P.E., Mogensen, K., Zuo, H., Monge-Sanz, B.M., 2019. SEAS5: the new ECMWF seasonal forecast system. Geosci. Model Dev. (GMD) 12, 1087–1117. https://doi.org/10.5194/gmd-12-1087-2019.

Kajtar, J., Holbrook, N., Hernaman, V., 2021. A catalogue of marine heatwave metrics and trends for the Australian region. Journal of Southern Hemisphere Earth Systems Science 71. https://doi.org/10.1071/ES21014.

Kajtar, J.B., Bachman, S.D., Holbrook, N.J., Pilo, G.S., 2022. Drivers, dynamics, and persistence of the 2017/2018 Tasman Sea marine heatwave. J. Geophys. Res.: Oceans 127, e2022JC018931. https://doi.org/10.1029/2022JC018931.

Kajtar, J.B., Holbrook, N.J., Lyth, A., Hobday, A.J., Mundy, C.N., Ugalde, S.C., 2024. A stakeholder-guided marine heatwave hazard index for fisheries and aquaculture. Clim. Change 177, 26. https://doi.org/10.1007/s10584-024-03684-8.

Knaff, J.A., Landsea, C.W., 1997. An El niño–southern oscillation climatology and persistence (CLIPER) forecasting scheme. Weather Forecast. 12, 633–652. https://doi.org/10.1175/1520-0434(1997)012<0633:AENOSO>2.0.CO;2.

Latif, M., Anderson, D., Barnett, T., Cane, M., Kleeman, R., Leetmaa, A., O'Brien, J., Rosati, A., Schneider, E., 1998. A review of the predictability and prediction of ENSO. J. Geophys. Res.: Oceans 103, 14375–14393. https://doi.org/10.1029/97JC03413.

Ma, J., Xu, H., Dong, C., Luo, J.-J., 2024. The forecast skills and predictability sources of marine heatwaves in the NUIST-cfs1.0 hindcasts. Adv. Atmos. Sci. 41, 1589–1600. https://doi.org/10.1007/s00376-023-3139-x.

Mason, S.J., Mimmack, G.M., 2002. Comparison of some statistical methods of probabilistic forecasting of ENSO. J. Clim. 15, 8–29. https://doi.org/10.1175/1520-0442(2002)015<0008:COSSMO>2.0.CO;2.

McAdam, R., Masina, S., Gualdi, S., 2023. Seasonal forecasting of subsurface marine heatwaves. Communications Earth Environment 4, 1–11. https://doi.org/10.1038/s43247-023-00892-5.

Mudelsee, M., 2019. Trend analysis of climate time series: a review of methods. Earth Sci. Rev. 190, 310–322. https://doi.org/10.1016/j.earscirev.2018.12.005.

Oliver, E.C.J., Benthuysen, J.A., Bindoff, N.L., Hobday, A.J., Holbrook, N.J., Mundy, C. N., Perkins-Kirkpatrick, S.E., 2017. The unprecedented 2015/16 Tasman Sea marine heatwave. Nat. Commun. 8, 16101. https://doi.org/10.1038/ncomms16101.

Oliver, E.C.J., Burrows, M.T., Donat, M.G., Sen Gupta, A., Alexander, L.V., Perkins-Kirkpatrick, S.E., Benthuysen, J.A., Hobday, A.J., Holbrook, N.J., Moore, P.J., Thomsen, M.S., Wernberg, T., Smale, D.A., 2019. Projected marine heatwaves in the 21st century and the potential for ecological impact. Front. Mar. Sci. 6, 734. https://doi.org/10.3389/fmars.2019.00734.

Oliver, E.C.J., Donat, M.G., Burrows, M.T., Moore, P.J., Smale, D.A., Alexander, L.V., Benthuysen, J.A., Feng, M., Sen Gupta, A., Hobday, A.J., Holbrook, N.J., Perkins-Kirkpatrick, S.E., Scannell, H.A., Straub, S.C., Wernberg, T., 2018. Longer and more frequent marine heatwaves over the past century. Nat. Commun. 9, 1324. https://doi.org/10.1038/s41467-018-03732-9.

Perkins-Kirkpatrick, S.E., King, A.D., Cougnon, E.A., Holbrook, N.J., Grose, M.R., Oliver, E.C.J., Lewis, S.C., Pourasghar, F., 2019. The role of natural variability and anthropogenic climate change in the 2017/18 Tasman Sea marine heatwave. Bull. Am. Meteorol. Soc. 100, S105–S110. https://doi.org/10.1175/BAMS-D-18-0116.1.

Ren, X., Liu, W., 2021. The role of a weakened atlantic meridional overturning circulation in modulating marine heatwaves in a warming climate. Geophys. Res. Lett. 48, e2021GL095941. https://doi.org/10.1029/2021GL095941.

Ren, X., Liu, W., Allen, R.J., Song, S.-Y., 2024. Distinct anthropogenic greenhouse gas and aerosol induced marine heatwaves. Environ. Res.: Climate 3, 015004. https://doi.org/10.1088/2752-5295/ad13ac.

Ren, X., Liu, W., Capotondi, A., Amaya, D.J., Holbrook, N.J., 2023. The Pacific Decadal Oscillation modulated marine heatwaves in the Northeast Pacific during past decades. Communication Earth Environment 4, 1–9. https://doi.org/10.1038/s43247-023-00863-w.

Smale, D.A., Wernberg, T., Oliver, E.C.J., Thomsen, M., Harvey, B.P., Straub, S.C., Burrows, M.T., Alexander, L.V., Benthuysen, J.A., Donat, M.G., Feng, M., Hobday, A. J., Holbrook, N.J., Perkins-Kirkpatrick, S.E., Scannell, H.A., Sen Gupta, A., Payne, B. L., Moore, P.J., 2019. Marine heatwaves threaten global biodiversity and the provision of ecosystem services. Nat. Clim. Change 9, 306–312. https://doi.org/10.1038/s41558-019-0412-1.

Smith, K.E., Burrows, M.T., Hobday, A.J., King, N.G., Moore, P.J., Sen Gupta, A., Thomsen, M.S., Wernberg, T., Smale, D.A., 2023. Biological impacts of marine heatwaves. Ann. Rev. Mar. Sci 15, 119–145. https://doi.org/10.1146/annurev-marine-032122-121437.

Smith, K.E., Burrows, M.T., Hobday, A.J., Sen Gupta, A., Moore, P.J., Thomsen, M., Wernberg, T., Smale, D.A., 2021. Socioeconomic impacts of marine heatwaves: global issues and opportunities. Science 374, eabj3593. https://doi.org/10.1126/science.abj3593.

Song, Y., Shu, Q., Bao, Y., Yang, X., Song, Z., 2021. The short-term climate prediction system FIO-CPS v2.0 and its prediction skill in ENSO. Front. Earth Sci. 9. https://doi.org/10.3389/feart.2021.759339.

Spillman, C., Smith, G., Hobday, A., Hartog, J., 2021. Onset and decline rates of marine heatwaves: global trends, seasonal forecasts and marine management. Frontiers in Climate 3. https://doi.org/10.3389/fclim.2021.801217.

Sun, W., Zhou, S., Yang, J., Gao, X., Ji, J., Dong, C., 2023. Artificial intelligence forecasting of marine heatwaves in the south China sea using a combined U-net and ConvLSTM system. Remote Sens. 15, 4068. https://doi.org/10.3390/rs15164068.